

High sensitivity neutron detector for Z

L. E. Ruggles,^{a)} J. L. Porter, Jr., W. W. Simpson, M. F. Vargas, and D. M. Zagar
Sandia National Laboratories, Albuquerque, New Mexico 87185-1193

R. Hartke, F. Buersegens, D. R. Symes, and T. Ditmire
The University of Texas at Austin, Austin, Texas 78712

(Presented on 19 April 2004; published 5 October 2004)

We have developed, calibrated, and tested a high sensitivity neutron detector that can be operated in the harsh x-ray bremsstrahlung environment that exists in experiments conducted on the 20 MA Z z-pinch facility located at Sandia National Laboratories in Albuquerque, New Mexico. The detector uses a scintillator coupled to a microchannel-plate photomultiplier tube detector and extensive x-ray shielding. © 2004 American Institute of Physics. [DOI: 10.1063/1.1789599]

I. DETECTOR DESCRIPTION

Recent experiments on the 20 MA, 100 ns rise-time Z z-pinch facility have demonstrated the potential for D–D fusion neutron production by inertial confinement fusion (ICF) capsule compression in the double-pinch vacuum hohlraum geometry.^{1,2} The hohlraum drive temperatures presently achievable with this target configuration, however, limit the expected isotropic neutron yield to $\leq 10^8$ neutrons. The need to systematically measure changes in yield caused by changing experimental parameters such as drive temperature, implosion asymmetries, and capsule surface roughness requires a neutron detector capable of measuring yields of as low as 10^6 neutrons for imperfect implosions. We have assembled and characterized an instrument with the goal of accurately measuring these low neutron yields in the harsh bremsstrahlung x-ray environment of Z.

The current-mode neutron detector³ assembled for this application consists of a scintillator and a microchannel plate photomultiplier tube (MCPMT). Detectors of this type rely upon a statistically significant number of neutron interactions in the scintillator producing a signal that is proportional to the total neutron yield. The solid angle viewed by the scintillator of the source, the scintillator thickness, the coupling efficiency of scintillator light to the MCPMT photocathode, the photocathode quantum efficiency, and the electron gain and transit time spread of the MCPMT must all be considered in the detector design.⁴

The scintillator, Saint Gobain type BC420 with 100 mm \times 25 mm front surface area located 900 mm from the imploding capsule, views 3.1×10^{-3} sr. The scintillator thickness of 75 mm matches the D–D neutron mean free path of 77 mm. The MCPMT, a Burle 85104-501, has a response time of about 2 ns which, when combined with the 1.3 ns response of the scintillator, produces a 2.5 ns single neutron response (Fig. 1). The neutron burn time is predicted to be significantly shorter than the detector response time. This fast system response time discriminates scattered neutrons with arrival time delays >5 ns from the prompt neu-

tron signal, and also produces a higher signal to noise ratio than a slower response detector with the same sensitivity.

The MCPMT is placed to one side of the scintillator to avoid exposure to x rays produced within the restricted line-of-sight of the detector (Fig. 2). A prism, coupled to the scintillator and MCPMT with index matching grease, reflects light from the scintillator onto the photocathode of the MCPMT. The efficiency of scintillator light onto the MCPMT photocathode is reduced in this arrangement in order to provide better shielding of the MCPMT from x rays. The MCPMT–prism–scintillator assembly, along with a power supply and diode laser alignment system, is sealed in an air-filled aluminum housing. The scintillator is coated with TiO₂ to improve the collection of scintillator light onto the MCPMT photocathode.

II. BREMSSTRAHLUNG SHIELD

There is a large high-energy x-ray background observed in experiments conducted on Z. The two major sources of this background are electron losses in the power flow electrodes and electron beams produced at the time of stagnation of the imploding z pinch. Electron losses at transmission line gaps produce 1–2 MeV endpoint bremsstrahlung at the beginning of current flow, and high energy electrons accel-

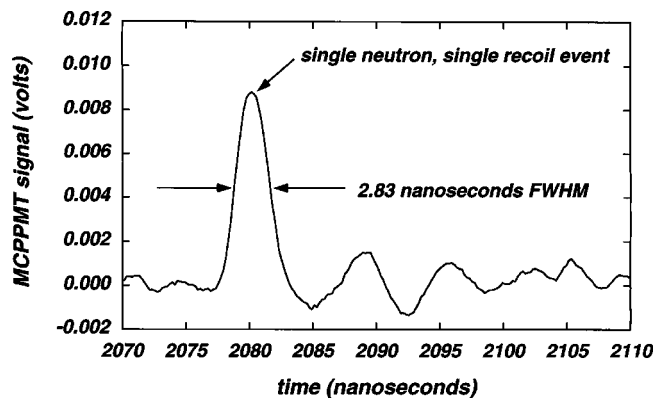


FIG. 1. Neutron detector signal from a single neutron, single recoil event. The post pulse oscillations are caused by an impedance mismatch between the MCPMT anode and the recording system.

^{a)}Electronic mail: leruggl@sandia.gov

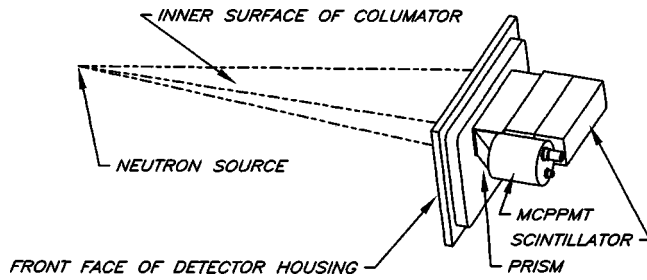


FIG. 2. A schematic illustrating the inner components of the neutron detector. An internal power supply, alignment laser, and the back and sides of the detector housing are removed in this view.

ated in the high dl/dt voltages generated in the z -pinch stagnation produce x rays up to 4 MeV in energy. The production of these x rays occurs 10–100 ns before capsule implosion and neutron production (Fig. 3). The integrated dose to a filtered array of CaF_2 thermoluminescent detectors from these high energy x rays has been measured and unfolded into a rough spectrum,⁵ and the amount of radiated x-ray energy above 1 MeV is estimated to be ≤ 800 J/sphere.

These high energy x rays can interact with both the scintillator and the microchannel plate in the photomultiplier tube to produce a large background signal. We have used a combination of extensive x-ray shielding and very good collimation to mitigate this problem by restricting the unattenuated field-of-view of the neutron detector to ≤ 3 mm surrounding the imploded capsule. This shielding technique is quite effective in reducing the x-ray background signal since the imploded capsule in the double-pinch inertial confinement fusion target design is separated from the imploding z -pinch plasma by ≥ 8 mm.

The detector shield has up to 54 cm of steel and 31 cm of tungsten between the scintillator and the pinch area, which effectively attenuates x rays of up to 4 MeV in energy. The double z -pinch geometry allows an opportunity for an almost unattenuated neutron flight path from the imploded capsule while severely attenuating high energy x rays generated in the transmission lines and the stagnated z -pinch plasma (Figs. 4 and 5).

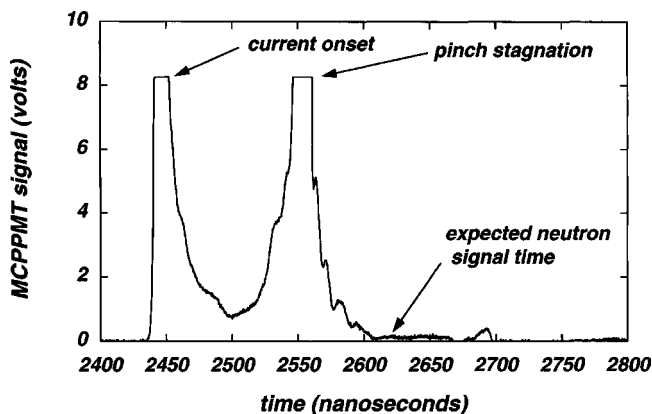


FIG. 3. Neutron detector output signal recorded on a Z double-pinch experiment showing the x-ray background signal that occurs at current onset and at pinch stagnation. Note that the output signal has returned to the baseline at the expected neutron arrival time.

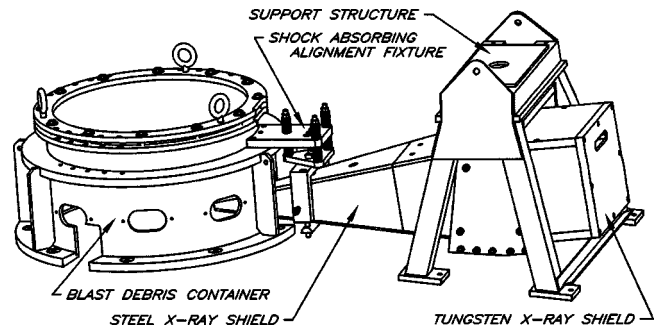


FIG. 4. A schematic illustrating the detector shield and support structure. The assembly rests on the Z transmission lines inside the Z vacuum vessel. The neutron detector (Fig. 2) is contained within the tungsten x-ray shield.

III. SINGLE NEUTRON SENSITIVITY

Although the scintillator and MCPMPT components of the neutron detector assembled here are well understood, large uncertainties in detection efficiency are caused by the physical details of collecting and coupling the scintillator light to the MCPMPT. In order to calibrate this detector, we measured its response to single neutrons by exposing the scintillator–MCPMPT assembly to a neutron source at The University of Texas at Austin.

The pulsed neutron source consists of a Ti:sapphire laser system producing a 40 fs, 250 mJ output pulse every 6 s focused onto D_2 gas clusters formed with a cryogenically cooled gas puff valve and nozzle. These clusters of a few hundred deuterium atoms explode with sufficient kinetic energy to produce $\sim 10^3$ – 10^5 D–D fusion neutrons per laser pulse.⁶ The source (produces very little bremsstrahlung).

The neutron detector, when placed at 2.0 m from the source, produced a signal on 643 of 7000 shots, ensuring that nearly all of the detected events were caused by a single neutron. A high bandwidth transient digitizer, triggered by the source plasma light, recorded the MCPMPT signals and provided time-of-flight information. X-ray and scattered neutron signals were identified by arrival time and discarded. The remaining signals were integrated and analyzed to obtain the average charge per pulse (Fig. 6).

The average charge determines the sensitivity of the detector to single neutrons (picoCoulombs/neutron), and the standard deviation indicates the statistical uncertainty above Poisson statistics.⁷ When the instrument is fielded on Z, the scintillator will interact with 245 ± 16 neutrons if the total isotropic yield is 10^6 neutrons, achieving $\sim 8\%$ statistical uncertainty in measuring the total yield. The expected detec-

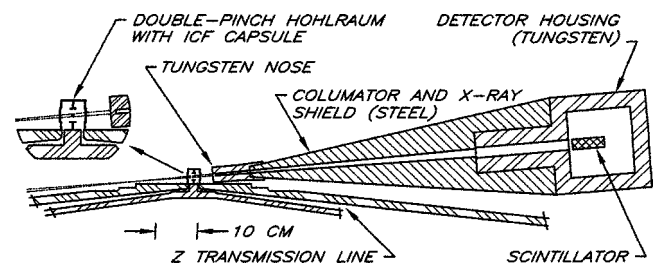


FIG. 5. A cross sectional view of the neutron detector x-ray shielding and collimation shows the detector's restricted field of view.

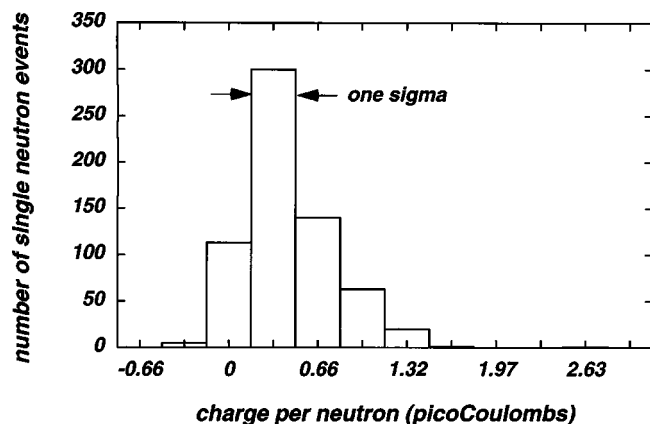


FIG. 6. Detector response to single neutrons. The statistical distribution of integrated pulses at an MCP-PMT bias of 2800 V indicates reasonable grouping. The median detected charge per neutron is 0.442 pC with a standard deviation of 0.330.

tor signal for 245 neutron interactions is 0.87 V (peak) at a 2800 V MCP-PMT bias if the detector response is assumed to be 4 ns full width at half maximum.

Because the detector sensitivity is dependent upon the MCP-PMT gain, we repeated the sensitivity measurement at higher MCP-PMT bias voltages and, although the statistics are not as good, the measured sensitivities agree with the normalized single-photoelectron MCP-PMT gain stated by the manufacturer (Fig. 7).

ACKNOWLEDGMENTS

Sandia is a multiprogram laboratory operated by Sandia Corporation, a Lockheed Martin Company, for the United

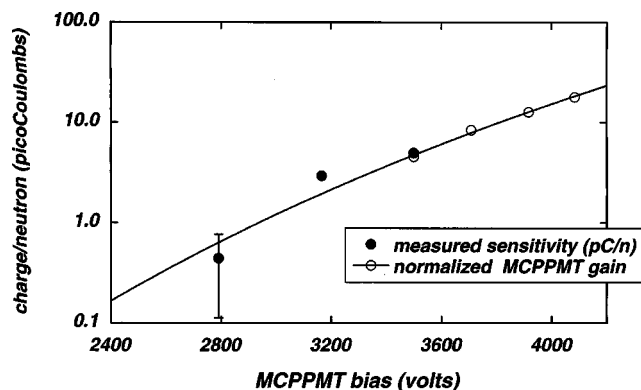


FIG. 7. Detector sensitivity plotted as a function of MCP-PMT gain. The manufacturers stated gain, when scaled, agrees well with the measured single neutron sensitivity. The error bar at 2800 V is the 1σ calibration uncertainty shown in Fig. 6.

States Department of Energy’s National Nuclear Security Administration under Contract No. DE-AC04-94AL8500.

¹R. A. Vesey *et al.*, *Phys. Plasmas* **10**, 1854 (2003).
²G. R. Bennett *et al.*, *Phys. Plasmas* **10**, 3717 (2003).
³T. J. Murphy *et al.*, *Rev. Sci. Instrum.* **72**, 775 (2001).
⁴R. E. Chrien, D. F. Simmons, and D. L. Holmberg, *Rev. Sci. Instrum.* **63**, 4886 (1992).
⁵D. H. Fehl, Sandia National Laboratories Internal Memorandum, “Fluence and time-integrated spectra from Bremsstrahlung near PBF-AZ,” April 1997.
⁶T. Ditmire, J. Zweiback, V. P. Yanovsky, T. E. Cowan, G. Hays, and K. B. Wharton, *Phys. Plasmas* **7**, 1993 (2000).
⁷T. J. Murphy, J. L. Jimerson, R. R. Berggren, J. R. Faulkner, J. A. Oertel, and P. J. Walsh, *Rev. Sci. Instrum.* **72**, 850 (2001).